EVALUATION OF THE DEFECT TOLERANCE OF PRESSURE VESSELS UNDER COMBINED THERMAL AND PRESSURE LOADS

I. MILNE

Central Electricity Generating Board, CERL, Kelvin Avenue, Leatherhead, Surrey KT22 7SE, United Kingdom

SUMMARY

A procedure is proposed which facilitates the assessment of the defect tolerance of structures subjected to combined secondary and primary loads using the failure assessment diagram used in the C.E.G.B., procedure 'Assessment of the Integrity of Structures Containing Defects'. The problem of defining the plasticity correction due to the secondary load in terms of the collapse load is overcome by separating the secondary load effects from those due to the primary load and plotting these along the K_r axis only. The resulting assessment point has coordinates

$$S_r = S_r^p$$

$$K_r = K_r^p + K_r^s + \rho$$

where the superscripts p and s infer primary and secondary loading and ρ is the correction required to K_r^s to allow for plasticity due to the secondary load only.

An example is presented to illustrate the use of the procedure for a combination of pressure and thermal loading.

1. Introduction

The procedures developed by Harrison, Loosemore and Milne [1] for failure analysis of structures work well for any stress level up to plastic collapse so long as the stress is derived from a primary load. Briefly, two calculations are required, one to evaluate how close the structure is to plastic collapse, S_r, the other to determine how close the structure is to linear elastic failure, K_r. Thus

$$S_r = \frac{\text{Load Applied}}{\text{Plastic Limit Load}} = \frac{\sigma}{\sigma_1(a/t)} \quad ; \quad K_r = \frac{\text{Load Applied}}{\text{LEFM Failure Load}} = \frac{K_1(\sigma, a/t)}{K_{1C}}$$

These two parameters are then entered as a coordinate point on a Failure Assessment Diagram (FAD), e.g. at A in Fig. 1, and the position of this point relative to the Failure Assessment Line (FAL) determines the factor of safety on load, F^L. Thus if K_{1C} is the cleavage fracture toughness, cleavage is predicted if $F^L \leqslant 1$. Alternatively if K_{1C} is defined at the initiation of ductile cracking, ductile crack initiation is predicted if $F^L \leqslant 1$. The need for, and the validity of this type of approach to failure assessment has been demonstrated many times [2,3,4]. In particular this approach is simple in concept and use, and facilitates a rapid sensitivity analysis on the input data and functions in such a way as to increase confidence in the predicted design or operating requirements of any structure [4].

In the presence of secondary loads, the situation is complicated by the fact that although they act like primary loads in LEFM they have no influence on the plastic limit load [5,6,7]. If secondary loads are treated like primary ones they can produce excessive underestimates of failure loads when they are tensile and excessive overestimates of failure loads when they are compressive. Moreover, since secondary loads can produce plasticity [8,9] the simple solution of including them algebraically in calculating K_r while ignoring them when calculating S_r is inadequate. A procedure has been developed by Chell [10] which solves this problem by renormalising the axes of the FAD to cater for any necessary plasticity corrections to the secondary load. However Chell's proposal complicates the analysis and the value of a simply constructed path to failure as a function of flaw size is lost. In the following a procedure simpler than that proposed by Chell is presented, and demonstrated using as an example a combination of thermal and pressure loading.

2. The Proposal

The FAL in Fig. 1 was derived from a model of yielding fracture mechanics [11] which relates the plastic zone size associated with a loaded crack to the crack opening displacement, or the elastic-plastic stress intensity factor, K_p, [12]. The FAL is thus a plot of the ratio of the elastic to the elastic plastic stress intensity factors, K_1/K_p, against S_r, with failure defined when $K_p = K_{1C}$ [10]. The procedures in [1] use the value of S_r to define the ratio K_1/K_p at failure, but of course, equally a ratio of K_1/K_p can be used to define an equivalent value of S_r.

Consider a secondary load applied to a structure which produces the ratio K_1^s/K_p^s at x in Fig. 2. This is equivalent to the value of S_r defined at A. If the ratio K_1^s/K_{1C} is defined at B in Fig. 2 then the coordinate point P, is the assessment point for this particular secondary load condition. Thus if $K_{1C} = K_p$ the point P would coincide with A. Moreover, any additional (tensile) loading would produce a new assessment point due to this loading only which fell within the shaded part of the diagram, with the S_r axis recalibrated as shown [10].

Consider now an additional primary load with values of S_r and K_r such that the resultant assessment point due to the combined loading falls on the FAL at O in Fig. 2. Failure is predicted and the safety factor on the primary load only, F^P, is unity. The co-ordinates of Q are defined in terms of the reduced diagram as $S_r = S_r^P$, $K_r = K_r^P + K_r^S$ and those of P as $S_r = O$, $K_r = K_r^S$. The dashed curve, LRM, is the original FAL redrawn on the new scale for S_r. The point R is vertically displaced from Q by a distance ρ^Q, and the point S from P a distance ρ^P which is equal to AL. Thus the above failure condition can be related to the original FAD by suitably adjusting the ordinate. The coordinates of R are thus $S_r = S_r^P$, $K_r = K_r^P + K_r^S + \rho^Q$ and those of S are $S_r = O$, $K_r = K_r^S + \rho^P$. In this way analysis can be made without redefining the S_r axis.

In Fig. 2 the value of ρ^P is different from the value of ρ^Q, as is generally the case as ρ varies with the value of S_r as shown in Fig. 3. To simplify the procedure, and maintain pessimism it is proposed to use the maximum value of ρ for any given ratio of K_1^S/K_p^S, and these are listed in Table 1.

3. Procedure for Secondary Loads

To perform an analysis, it is first necessary to evaluate the ratio K_1^S/K_p^S for the given loading and flaw size. A simple plastic zone size correction η is sufficient for this and any appropriate constraint factor can be easily included. Chell [10] proposed a value of $\eta = \pi/16\ (K_1/\sigma_y)^2$ for plane strain conditions and $\eta = \pi/8\ (K_1/\sigma_y)^2$ for plane stress, well in excess of the normally accepted plastic zone size corrections. Thus together with the use of the maximum value of ρ the analysis can be guaranteed to be satisfactorily pessimistic.

The procedure is thus as follows:-

1. Make a plot of K_1^S against flaw size
2. Evaluate η. For plane stress constraint use $\eta = \pi/8\ (K_1^S/\sigma_y)^2$ and for plane strain $\eta = \pi/16\ (K_1^S/\sigma_y)^2$.
3. Evaluate the ratio K_1^S/K_p^S. For the flaw size of interest, a, this can be obtained from the above plot as $K_1^S/K_p^S = K_1^S(a)/K_p^S(a+\eta)$.
4. Determine the necessary value of ρ from Table 1. Note that where the gradient of K_1^S is negative the ratio K_1^S/K_p^S is greater than 1. In such cases, pessimism will be maintained by taking $\rho = O$.

5. Example

A pressure vessel is considered to have a semi-circular flaw at the inner surface of its 10mm thick membrane region. Under nominal operating conditions the load on the vessel consists of a pressure stress of 186.6 MPa and a thermally induced secondary stress with a profile shown in Fig. 4. The fracture toughness is uniform across the section at 120 MPa$\sqrt{m}$, the value for the initiation of ductile cracking. During cool down the secondary stress field remains unchanged while the fracture toughness at the inner surface of the membrane decreases to $\sim$ 60MPa$\sqrt{m}$. In the following the proposed procedure is used to demonstrate how to determine the relative integrity of the structure under the above conditions of operation.

(a) Flaw Mode. The flaw size, a/t, is variable with t = 110mm. $a/\ell = 0.5$ (Fig. 4).

(b) Loading. The pressure (primary) stress, σ^P, is 186.6 MPa and regarded as uniform through the thickness. The thermal (secondary) stress profile is as shown in Fig. 4.

(c) Material Properties. Yield and ultimate tensile stresses are not less than 420 and 580 MPa, so the flow stress, $\bar{\sigma}$, is taken as 500 MPa, and is temperature independant over the range of interest. Under normal (hot) operation the fracture toughness, K_{1C}, is

120 MNa$\sqrt{m}$. During cool-down a toughness profile is set up as shown in Fig. 4.

(d) Procedure.

(i) $$S_r = \frac{\sigma^P}{\bar{\sigma}(1-{}^c/w)} = \frac{0.37}{(1-{}^c/w)}$$

where ${}^c/w$ is evaluated to take account of the flaw ellipticity ${}^a/\ell$, from Fig. 5 [4].

(ii) $$K_r^P = \frac{K_1^P}{K_{1C}}$$

Values for K_1^P were obtained at $\beta = 0^o$ and 90^o, Fig. 4, using the computer program FRACPAC [13].

(iii) $$K_r^{th} = \frac{K_1^{th}}{K_{1C}}$$

Again FRACPAC was used to determine K_1^{th} and the resulting values are plotted in Fig. 6 as a function of flaw depth a.

(iv) To determine ρ, η was taken as ${}^\pi/16(K_1^{th}/\sigma_y)^2$ at $\beta = 0^o$, and as ${}^\pi/8(K_1^{th}/\sigma_y)^2$ at $\beta = 90^o$. The ratio $K_1^{th}/K_p^{th} = K_1^{th}(a)/K_1^{th}(a+\eta)$ was then determined from Fig. 6 for each flaw size of interest. Table 2 lists the resulting values of ρ. K_r^o is the value of K_r under zero pressure, and this parameter is needed to establish the safety factors on pressure, F^P.

(e) Analysis. In Table 2 the coordinates for the FAD are listed for different flaw depths, a, and these are plotted on Figs. 7a and b. The open symbols represent ductile initiation while the closed symbols are for cleavage failure. It is clear from these Figures that the risk of failure is largest during cooldown, that the location on the flaw at the inner surface of the vessel at $\beta = 90^o$, is the most vulnerable one. Failure here would be by cleavage.

The safety factors on pressure, F^P, were calculated as demonstrated for a = 44mm at $\beta = 90^o$ in Fig. 7b, and are listed in Table 3. This shows, for example, that a 44mm deep flaw would remain stable during cooldown, if the pressure was first reduced to 0.69 of the normal operating pressure.

5. Discussion and Conclusion

The procedures proposed are simple, satisfactorily pessimistic and yet predict the type of behaviour which has been both experimentally observed [7] and theoretically predicted [6,8,9] when structures are loaded by a combination of secondary and primary loads. Thus

(1) Under secondary loading only, failure is predicted when the plastically corrected stress intensity factor exceeds K_{1C}, i.e. when $K_r^S + \rho > 1$.

(2) Under primary loading only, failure is as predicted by the procedures in [1].

(3) Under combined loading failure in the collapse limit is not affected by the secondary load, but failure in other regimes is affected by this secondary load, algebraically. So the normal principles of fracture mechanics are satisfied while retaining the many advantages of the failure route [1].

By separating the primary and secondary load effects the procedure facilitates judgement of safety factors on primary loads only, a useful attribute, since primary loads tend to be more controllable than secondary ones. Thus they can be used to determine any modifications in operating regime which may be needed for safe operation.

In the example presented, under normal (hot) operation there is little risk of failure for moderately sized defects. During cool-down however, the resultant gradient in K_{1C} reduces the safety factors, especially where the flaw interacts with the inner surface of the vessel, at $\beta = 90^{o}$, even though the thermal stress gradient is comparatively modest. A more severe thermal stress field, of the type which might occur under a fault condition, would be expected to exaggerate this effect.

It is worth emphasising the additional use to which an analysis of this type can be put. Because of the restrictions imposed by the two limiting criteria at $K_r = 1$ and $S_r = 1$ confidence in the analysis technique is fundamentally very high. There is however a great benefit to be had in performing a sensitivity analysis on the most unreliable of the input data, and this of course can be performed very easily [4]. Confidence will be even further increased if it can be shown that, for example, large changes in K_{1C} have little effect on the predicted safety factors for the flaw sizes of interest.

6. Acknowledgements

This work was performed at the Central Electricity Research Laboratories and is published by permission of the Central Electricity Generating Board.

7. References

[1] Harrison, R.P., Loosemore, K. and Milne, I., C.E.G.B. report R/H/R6 (1976)

[2] Dowling, A.R. and Townley, K.H.A., Int. J. of Pressure Vessels and Piping 3 77 (1975)

[3] Harrison, R.P., Loosemore, K. and Milne, I., SMIRT 4 G2/d (1977)

[4] Milne, I., Loosemore, K. and Harrison, R.P., Conference on Tolerance of Flaws in Pressurized Components paper C106/78, London 1978.

[5] Townley, C.H.A., Int. J. of Pressure Vessels and Piping 4 207 (1976)

[6] Chell, G.G. and Ewing, D.J.F., C.E.G.B. Report RD/L/N216/76 (1977)

[7] Formby, C.L. and Griffiths, J.R., Int. Conf. on Residual Stresses in Welded Construction and Their Effects (1978)

[8] Heaton, A., C.E.G.B. Report NW/SSD/RR 158/76 (1976)

[9] Ainsworth, R.A., Neale, B.K. and Price, R.H., Conference on Tolerance of Flaws in Pressurized Components paper C96/78, London (1978)

[10] Chell, G.G., ASTM E24 Meeting on Elastic Plastic Fracture, Atlanta (1977) ASTM STP668

[11] Bilby, B.A., Cottrell, A.H. and Swinden, K.W., Proc. Roy. Soc. A272 304 (1963)

[12] Heald, P.T., Spink, G.M., and Worthington, P.J. Mat. Sci. and Engng. 10 129 (1972)

[13] Chell, G.G., "FRACPAC" CEGB report RD/L/N 170/77 (1978)

TABLE 3: Safety Factors on Pressure, F^{p}

a (mm)	F^{p} when hot		F^{p} on Cool-Down	
	$\beta=0^{o}$	$\beta=90^{o}$	$\beta=0^{o}$	$\beta=90^{o}$
5.5	2.73	2.68	2.48	2.08
11.0	2.65	2.47	2.24	1.53
22.0	2.33	2.10	2.11	1.05
33.0	2.07	1.80	2.07	0.83
44.0	1.86	1.61	1.86	0.69

TABLE 1

$K_1^s(a)$ / $K_1^s(a+\eta)$	0.00	0.01	0.02	0.03	0.04	0.05	0.06	0.07	0.08	0.09	0.10
	Plasticity Correction to K_r^s, ρ										
0.0	1.000	0.990	0.980	0.970	0.960	0.950	0.940	0.930	0.920	0.910	0.900
0.1	0.900	0.890	0.880	0.870	0.860	0.850	0.840	0.830	0.820	0.810	0.800
0.2	0.800	0.790	0.780	0.770	0.760	0.750	0.740	0.730	0.720	0.710	0.700
0.3	0.700	0.690	0.680	0.670	0.660	0.650	0.640	0.630	0.620	0.610	0.600
0.4	0.600	0.590	0.580	0.570	0.560	0.550	0.540	0.530	0.520	0.510	0.500
0.5	0.500	0.490	0.480	0.470	0.460	0.450	0.440	0.430	0.420	0.411	0.402
0.6	0.402	0.392	0.383	0.374	0.366	0.358	0.350	0.342	0.333	0.325	0.316
0.7	0.316	0.307	0.299	0.291	0.282	0.274	0.265	0.257	0.248	0.240	0.231
0.8	0.231	0.222	0.213	0.204	0.195	0.186	0.177	0.168	0.159	0.149	0.140
0.9	0.140	0.130	0.119	0.109	0.098	0.086	0.075	0.063	0.048	0.030	0.000

TABLE 2

a (mm)	K_1^{th} ($MPa\sqrt{m}$)	η (mm)	K_1^{th}/K_p^{th}	ρ	K_1^p ($MPa\sqrt{m}$)	Hot Operation			Cool Down			S_r	Location on Flaw
						K_{1C} ($MPa\sqrt{m}$)	K_r^o	K_r	K_{1C} ($MPa\sqrt{m}$)	K_r^o	K_r		
5.5	6.5	-	1	0	16.2	120	0.05	0.19	67	0.10	0.34	0.37	$\beta = 0^o$
11.0	8.2	-	"	"	23.0	"	0.07	0.26	77	0.11	0.41	0.37	
22.0	8.8	-	"	"	32.6	"	0.07	0.34	99	0.09	0.42	0.39	
33.0	7.7	-	"	"	40.0	"	0.06	0.40	120	0.06	0.40	0.41	
44.0	5.9	-	"	"	46.4	"	0.05	0.44	120	0.05	0.44	0.46	
5.5	8.4	.15	.99	.03	19.1	120	0.10	0.26	60	0.17	0.49	0.37	$\beta = 90^o$
11.0	11.6	.30	.98	.048	27.0	"	0.15	0.38	"	0.24	0.69	0.37	
22.0	15.5	.53	.99	.03	38.3	"	0.16	0.48	"	0.29	0.93	0.37	
33.0	17.9	.71	.99	.03	46.9	"	0.18	0.57	"	0.33	1.11	0.37	
44.0	19.6	.86	.99	.03	54.1	"	0.19	0.64	"	0.36	1.26	0.37	

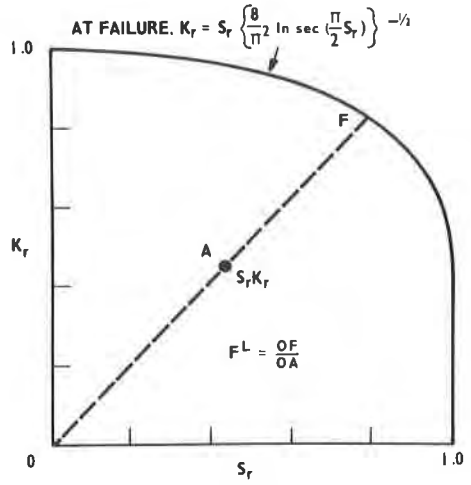

FIG. 1

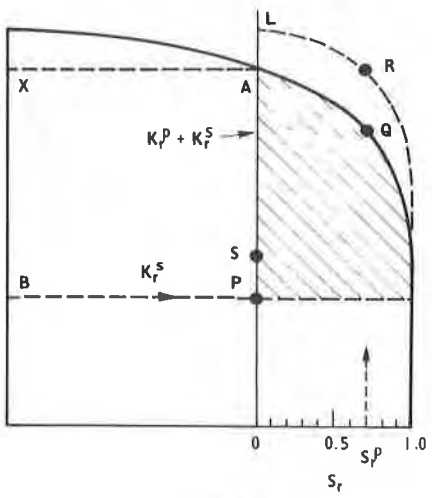

FIG. 2

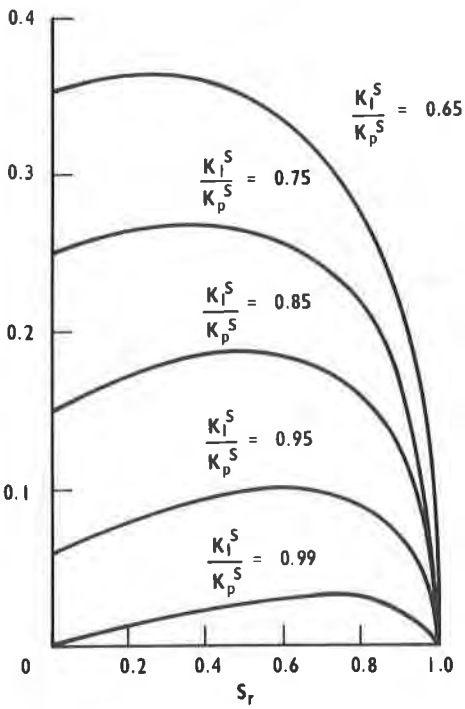

FIG. 3

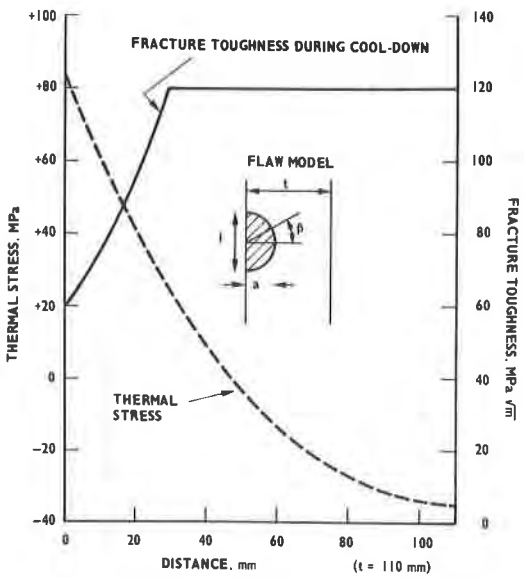

FIG. 4

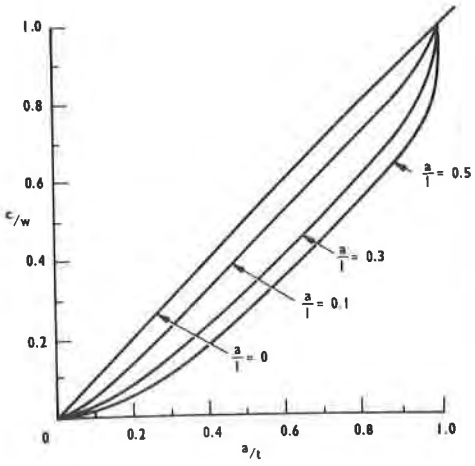

FIG. 5

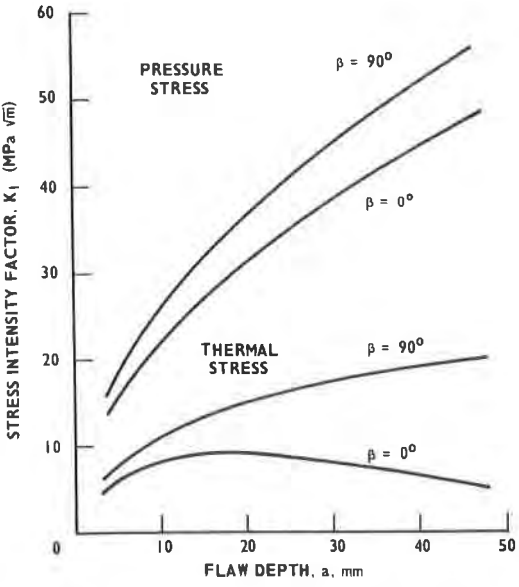

FIG. 6

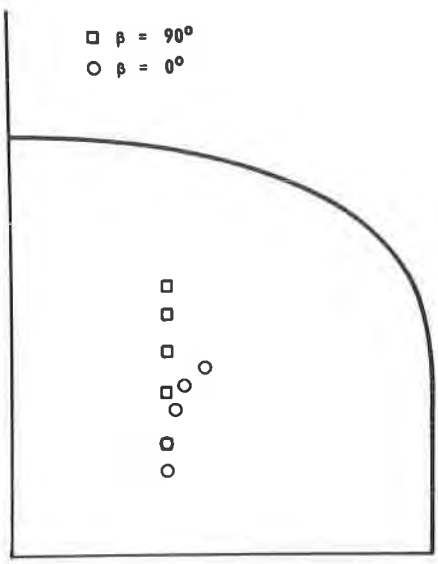

FIG. 7(a) NORMAL OPERATION (HOT)

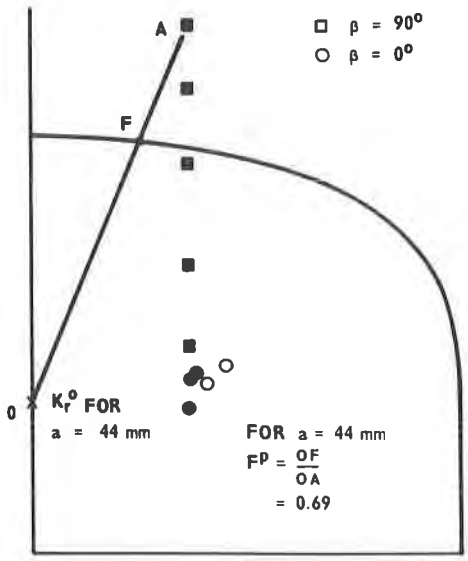

FIG. 7(b) COOL-DOWN